SUSY SEARCHES WITH THE ATLAS EXPERIMENT*

Paweł Klimek

on behalf of the ATLAS Collaboration

Northern Illinois University
DeKalb, IL 60115, United States

(Received April 12, 2016)

The Standard Model describes the elementary particles and their interactions. Supersymmetry, a symmetry beyond those included in the Standard Model, could resolve some of its shortcomings. Supersymmetry can provide a solution to the hierarchy problem and a candidate for dark matter. The Large Hadron Collider has the potential to produce some of the particles predicted by supersymmetry. This document presents searches for supersymmetric particles in proton–proton collision data recorded by the ATLAS experiment. The analyses are done using $\mathscr{L} = 3.2$ fb^{-1} proton–proton collisions at $\sqrt{s} = 13$ TeV collected in 2015. Also, searches performed using up to $\mathscr{L} = 20.3$ fb^{-1} dataset at $\sqrt{s} = 7$ and 8 TeV collected in 2011 and 2012 are presented.

DOI:10.5506/APhysPolB.47.1505

1. Introduction

Currently, the best description of particle physics phenomena is given by the Standard Model (SM). The SM has been extensively tested during the last four decades and has shown great predictive power. However, there are observed phenomena that are not explained by the Standard Model. The answers to several questions are sought: How can a quantum field theory of gravitation be formulated? What is dark matter and dark energy? What is the origin of neutrino masses? Why mass of Higgs boson is so low? Therefore, a new theory is needed. One of the theories tested with ATLAS is supersymmetry (SUSY) [1–12] which is also the main subject of this document.

* Presented at the Cracow Epiphany Conference on the Physics in LHC Run 2, Kraków, Poland, January 7–9, 2016.

A supersymmetric transformation turns a bosonic state into a fermionic one and *vice versa*. In this way, every Standard Model particle has a supersymmetric partner called a superpartner. Some SUSY models can have more than one superpartner per SM particle. The supersymmetric partner has all quantum numbers and couplings equal to its Standard Model counterpart except for the spin, which differs by 1/2. Every SM fermion (with spin 1/2) has a spin 0 superpartner. Similarly, every SM gauge boson (with spin 1) has a superpartner with spin 1/2. The physical superpartners of the SM particles are scalar partners of quarks and leptons (squarks ($\tilde{q}$) and sleptons ($\tilde{l}$)), fermionic partners of gauge and Higgs bosons (gluinos ($\tilde{g}$), charginos ($\tilde{\chi}^{\pm}$) and neutralinos ($\tilde{\chi}^{0}$)). The charginos and neutralinos are mixtures of the wino, bino and higgsino that are superpartners of the electroweak gauge bosons W^i, B and the Higgs boson, respectively. Their mass eigenstates are referred to as $\tilde{\chi}_i^{\pm}$ $(i = 1, 2)$ and $\tilde{\chi}_j^0$ $(j = 1, 2, 3, 4)$ in order of increasing mass. The superpartner of the gluon is gluino.

If Nature was exactly supersymmetric, all the superpartners would have the same mass as their Standard Model partners. Since no such particles have been observed to date, the mass of the superpartners has to be larger than the mass of SM partners. Therefore, supersymmetry, if it is a theory describing Nature, must be broken.

In SUSY models with R-parity conservation [13–16], the supersymmetric particles are produced in pairs. An absolutely stable lightest supersymmetric particle (LSP) with no electric charge nor colour charge interacting only weakly and gravitationally, is an excellent weakly interacting massive particle (WIMP) dark mater candidate. If the sparticle masses are not much larger than 1 TeV, SUSY can solve the hierarchy problem [17–24]. The SM particles and their superpartners have cancelling contributions to the radiative corrections to the Higgs mass. An unnatural fine tuning is not needed and the hierarchy problem is elegantly solved in the presence of supersymmetric particles.

This document presents ATLAS studies of several classes of simplified models and phenomenological minimal supersymmetric Standard Model (pMSSM) [25–27]. The models considered assume R-parity conservation and $\tilde{\chi}_1^0$ as the LSP. Different combinations of physics objects in the final state are covered. Early Run 2 studies using first $\mathscr{L} = 3.2$ fb^{-1} at $\sqrt{s} = 13$ TeV are presented. Few examples of the rich variety of Run 1 results at $\sqrt{s} = 7$ and 8 TeV using a total integrated luminosity up to $\mathscr{L} = 20.3$ fb^{-1} are also shown giving emphasis to the most recent results.

The document is organized as follows: Section 2 provides a brief description of the ATLAS detector, Section 3 presents inclusive strong production searches, Section 4 is dedicated to third generation squark direct production

searches and Section 5 to electroweak production searches, Section 6 shows the interpretation of the SUSY searches in the pMSSM, finally, conclusions are drawn in Section 7.

2. The ATLAS detector

The ATLAS experiment [28] is a general purpose detector designed to study processes that take place in collisions at the Large Hadron Collider (LHC) [29]. Its goal is to make precise measurements of fundamental quantities and search for new physics phenomena, such as new particles and new interactions. The ATLAS detector has a cylindrical shape around the beam pipe axis and nearly 4π coverage in solid angle. It consists of several concentric subdetectors. The inner tracking detector (ID) covers the pseudorapidity[1] region $|\eta| < 2.5$ and consists of a silicon pixel detector, a semiconductor microstrip detector, and a transition radiation tracker. The ID is surrounded by a thin superconducting solenoid providing a 2 T axial magnetic field. A high-granularity lead/liquid-argon sampling calorimeter measures the energy and the position of electromagnetic showers within $|\eta| < 3.2$. An iron-scintillator tile calorimeter measures hadronic showers in the central region ($|\eta| < 1.7$). The end-cap ($1.5 < |\eta| < 3.2$) and forward ($3.1 < |\eta| < 4.9$) regions are instrumented with LAr calorimeters to measure both electromagnetic and hadronic showers. The muon spectrometer (MS) surrounds the calorimeters and consists of three large superconducting air-core toroid magnets, each with eight coils, a system of precision tracking chambers ($|\eta| < 2.7$) and fast trigger chambers ($|\eta| < 2.4$). The trigger system [30] selects events to be recorded for off-line analysis.

3. Inclusive strong production searches

This section presents several results from inclusive searches for strongly produced gluinos and first and second generation squarks using $\mathscr{L} = 3.2\ \text{fb}^{-1}$ dataset at $\sqrt{s} = 13$ TeV. These SUSY particles (sparticles) are expected to have high cross section for masses up to around 1 TeV. The considered models assume the decay of the SUSY particles to $\tilde{\chi}_1^0$, which will escape the experiment undetected. The decay chain leading from the strongly produced sparticles to the LSP will involve the production of a number of SM particles, predominantly hadronic jets and, depending on the scenario, sometimes leptons. The escaping LSP provides a source of missing transverse momentum (whose magnitude is referred to as $E_{\text{T}}^{\text{miss}}$), a requirement which is also

[1] ATLAS uses a right-handed coordinate system with its origin at the nominal interaction point (IP) in the centre of the detector and the z-axis along the beam pipe. The x-axis points from the IP to the centre of the LHC ring, and the y-axis points upward. Cylindrical coordinates (r, ϕ) are used in the transverse plane, ϕ being the azimuthal angle around the beam pipe. The pseudorapidity is defined in terms of the polar angle θ as $\eta = -\ln\tan(\theta/2)$.

commonly included in searches. A wide range of final states is investigated. A multitude of signal regions have been designed to probe different parts of the phase space using different cuts on the number of jets, the number of charged light leptons (electrons or muons), and the transverse momenta of all particles and jets in the event.

A search for squarks and gluinos in final states containing jets (≥ 2 to ≥ 6 jets), $E_{\mathrm{T}}^{\mathrm{miss}}$ and no electrons or muons has been performed [31]. Because of the high mass scale expected for the SUSY signal, the scalar sum of the transverse momenta of jets and $E_{\mathrm{T}}^{\mathrm{miss}}$ is a powerful discriminant between the signal and most SM backgrounds. Figure 1 illustrates the squark- and gluino-pair production, followed by the direct decays of squarks (a) and direct (b) or chargino mediated (c) decays of gluinos considered in this work. Good agreement is seen between the numbers of events observed in the data

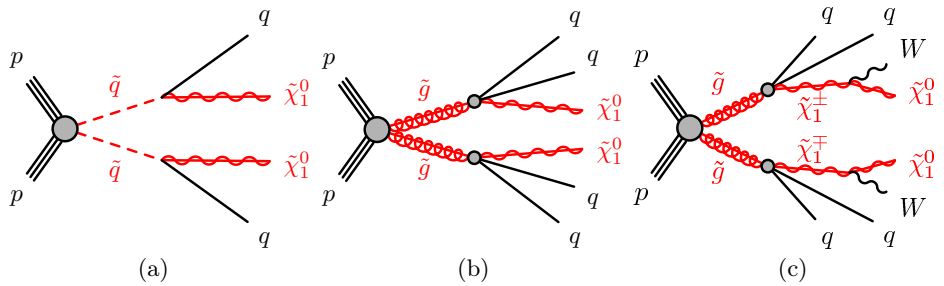

Fig. 1. Illustration of squark pair production (a), gluino pair production (b) and (c) subsequent direct decay of squarks and direct or one-step decays of gluinos. Taken from Ref. [31].

and those expected from SM processes. Results are interpreted in terms of simplified models with only light-flavour squarks or gluinos, together with a neutralino LSP, with the masses of all the other SUSY particles set beyond the reach of the LHC. In Fig. 2, limits at 95% confidence level (C.L.) are shown for two classes of simplified model in which only direct production of light-flavour squark (a) or gluino (b) pairs decaying directly to SM particles are considered. In these simplified model scenarios, the lower limit on the light-flavour squark mass is 980 GeV assuming massless $\tilde{\chi}_1^0$. The corresponding limit on the gluino mass is 1520 GeV, when the $\tilde{\chi}_1^0$ is massless. In Fig. 2 (c), limits are shown for pair-produced gluino each decaying via an intermediate $\tilde{\chi}_1^{\pm}$ to two quarks, a W boson and a $\tilde{\chi}_1^0$. Results are presented for simplified models in which the mass splitting between the $\tilde{\chi}_1^{\pm}$ and the $\tilde{\chi}_1^0$ is related to that between the gluino and the $\tilde{\chi}_1^{\pm}$, and is fixed to $m_{\tilde{\chi}_1^{\pm}} = (m_{\tilde{g}}+m_{\tilde{\chi}_1^0})/2$. In this model, for a $\tilde{\chi}_1^0$ mass of 200 GeV, the lower limit on the gluino mass is 1510 GeV. These results extend the region of supersymmetric parameter space excluded by previous ATLAS searches that are also shown.

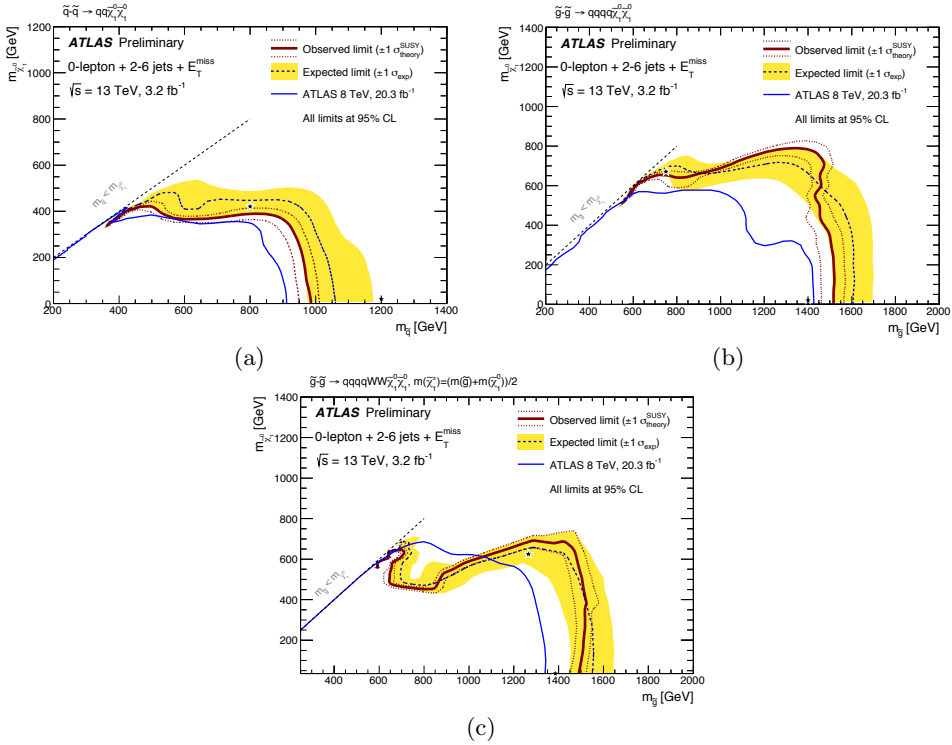

Fig. 2. (Colour on-line) 95% C.L. exclusion limits for direct production of light-flavour squark pairs decaying to one quark and $\tilde{\chi}_1^0$ with decoupled gluinos (a), gluino pairs decaying to two quarks and $\tilde{\chi}_1^0$ with decoupled squarks (b) and gluino pairs decaying via an intermediate $\tilde{\chi}_1^0$ to two quarks, a W boson and a $\tilde{\chi}_1^0$ for models with a fixed $m_{\tilde{\chi}_1^\pm} = (m_{\tilde{g}} + m_{\tilde{\chi}_1^0})/2$ (c). The dashed (blue) lines show the expected limits at 95% C.L., with the grey (yellow) bands indicating the 1σ excursions due to experimental and background-only theoretical uncertainties. Observed limits are indicated by thick black (maroon) curves where the solid contour represents the nominal limit, and the dotted lines are obtained by varying the signal cross section by the theoretical uncertainties. Results are compared with the observed limits obtained by Run 1 ATLAS search. Taken from Ref. [31].

The next work concerns a search for gluinos in final states with large jet multiplicities and $E_{\mathrm{T}}^{\mathrm{miss}}$ [32]. Events with various jet multiplicities (≥ 7 to ≥ 10 jets) and with various b-jet multiplicity requirements (≥ 0, ≥ 1 and ≥ 2 b-tagged jets) are selected to enhance sensitivity. In contrast to many other searches for the production of strongly interacting SUSY particles, the requirement of large jet multiplicity made here means that the requirement on $E_{\mathrm{T}}^{\mathrm{miss}}$ can be modest. No excess above SM expectations is observed. The results are interpreted within two supersymmetry models. The first is a

simplified model, the second is drawn from a two-dimensional subspace of the 19-parameter pMSSM. In both models, gluinos are pair-produced and then decay via the cascade to heavy SM particles, such as W and Z bosons, each of which can produce multiple jets in their decays. Figure 3 (a) shows the topology of the simplified model considered in this search. The most

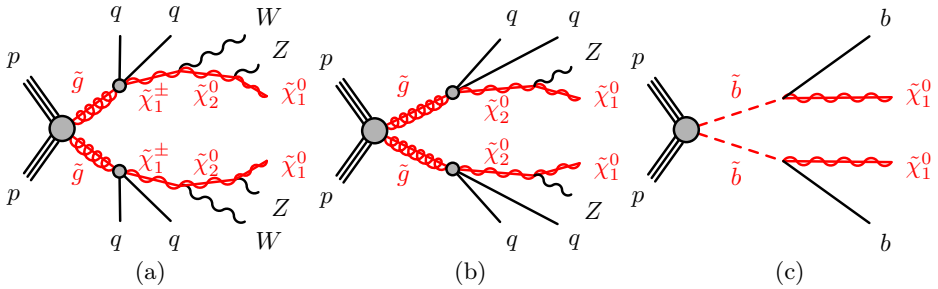

Fig. 3. Illustration of gluino pair production and subsequent two-step decay (a), gluino pair production and subsequent effective three-body decay (b) [33], and bottom squark pair production and subsequent direct decay (c) [34].

sensitive signal regions are found to be those with no b-jet requirement for the simplified model decay. For the pMSSM slice, which has large branching ratios for gluinos to third-generation quarks, the best signal regions are those requiring either one or two b-jets. Figure 4 shows the limits for pMSSM (a) and simplified model (b). In both cases, gluino masses up to 1400 GeV are excluded at 95% C.L., significantly extending previous limits for the simplified model decay.

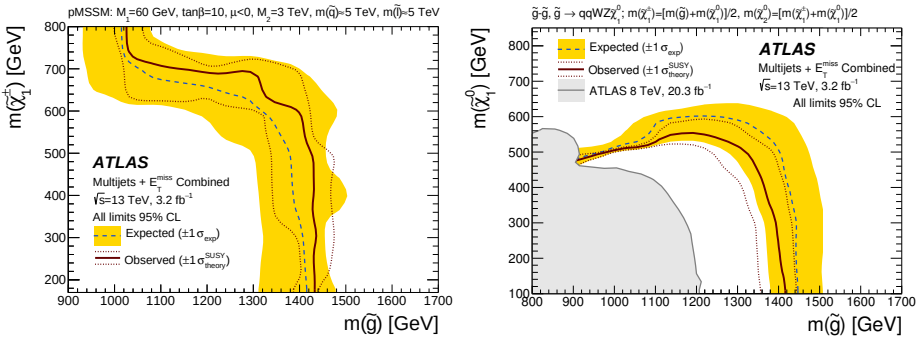

Fig. 4. 95% C.L. exclusion limits for direct production of gluino pairs decaying via the cascade for pMSSM (a) with respect to the gluino mass ($m_{\tilde{g}}$) and to the chargino mass ($m_{\tilde{\chi}_1^\pm}$), and for simplified model (b) with respect to the gluino mass and to the neutralino mass ($m_{\tilde{\chi}_1^0}$). Results are compared with the observed limits obtained by Run 1 ATLAS searches. Taken from Ref. [32].

Another of the many interesting searches performed in the frame of the strong production searches is the analysis where events are required to contain at least two the same-flavour leptons (electrons or muons), with opposite charge, coming from the decay of a Z boson, at least two jets and large $E_{\mathrm{T}}^{\mathrm{miss}}$ [33]. Figure 3 (b) shows the topology of the simplified model considered in this search. After using data-driven methods to estimate all major backgrounds, which are thoroughly cross checked with other methods (including data-driven and MC), the total background estimated in signal region (SR) is 10.3 ± 2.3 events, whereas the observed number of events is 21. This excess corresponds to a significance of 2.2 standard deviations. Figure 5 shows the number of observed events contrasted with the estimated background in all validation regions (VR) and in the SR considered in the analysis. This plot is especially interesting since it shows that the excess is not an effect of the incorrect estimation of backgrounds. As it can be seen, in all the validation regions, the observed and estimated number of events are in very good agreement. It is worth mentioning that the same search performed by ATLAS in $\mathscr{L} = 20.3\ \mathrm{fb}^{-1}$ at $\sqrt{s} = 8$ TeV had found an excess of events above the SM background with a significance of 3 standard deviations. More Run 2 data is necessary in order to answer the question if this excess was a hint of new physics or a statistical fluctuation.

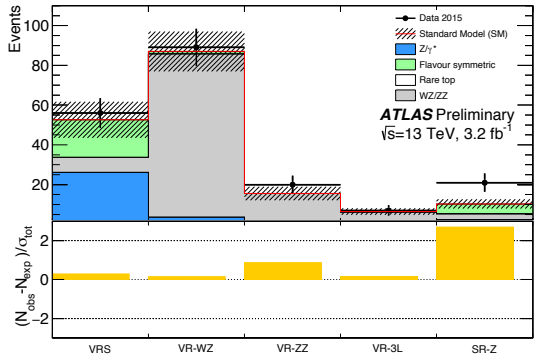

Fig. 5. The observed and expected yields in the validation regions and signal region in analysis devoted to SUSY search in events containing a leptonically decaying Z boson, jets and $E_{\mathrm{T}}^{\mathrm{miss}}$. The lower panel shows the difference in standard deviations between the observed and expected yields. Taken from Ref. [33].

Next analysis concerns search for pair production of gluinos decaying via sbottom (Gbb model) and stop (Gtt model) to the lightest neutralino [35]. Diagrams of the simplified models considered are shown in Fig. 6 (a) and (b). The sbottom and stop are assumed to be produced off-shell such that the gluinos undergo the three-body decay and that the only parameters of the simplified models are the gluino and neutralino masses. The signal is searched

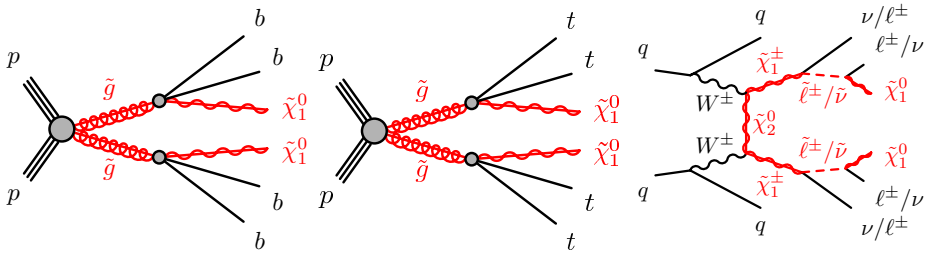

Fig. 6. Illustration of gluino pair production and subsequent decay into bottom quarks in Gbb (a) and into top quarks in Gtt simplified models (b) [35]. Illustration of the same sign $\tilde{\chi}_1^{\pm}\tilde{\chi}_1^{\pm}$ pair production via vector boson fusion and subsequent decay with intermediate light charged sleptons and sneutrinos (c) [36]. All three slepton generations are included in the definition of $\tilde{\ell}/\tilde{\nu}$.

for in events containing several energetic jets, of which at least three must be identified as b-jets, large $E_{\mathrm{T}}^{\mathrm{miss}}$ and either zero or at least one charged lepton. Massive large-radius jets are also used to identify highly boosted top quarks. The data are found to be in good agreement with the predicted background yield. The 95% C.L. excluded limits for the Gbb and Gtt models are shown in the LSP and gluino mass plane in Fig. 7 (a) and (b), respectively. For the Gbb model, gluinos with masses below approximately 1780 GeV are excluded at 95% C.L. for LSP masses below 800 GeV. The best exclusion limit on the LSP mass is 925 GeV, which is reached for a range of gluino masses between approximately 1200 GeV and 1600 GeV. For the Gtt model, gluino masses up to 1710 GeV are excluded for massless LSP. For LSP masses below 700 GeV, gluino masses below approximately 1675 GeV are excluded. The

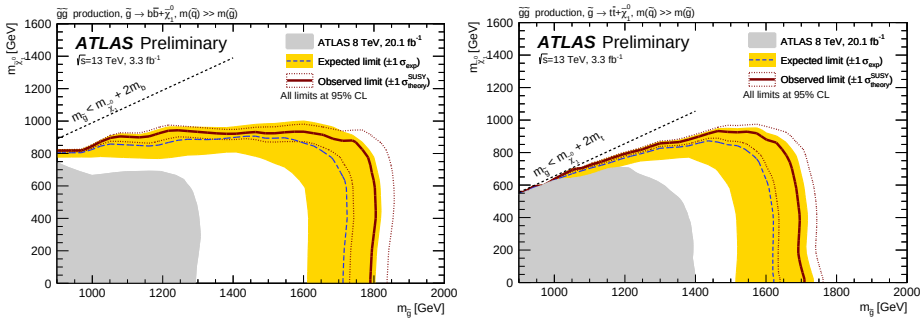

Fig. 7. 95% C.L. exclusion limits for direct production of gluinos decaying to bottom quarks in Gbb (a) and to top quarks in Gtt simplified models (b) with respect to the gluino mass ($m_{\tilde{g}}$) and to the neutralino mass ($m_{\tilde{\chi}_1^0}$). Results are compared with the observed limits obtained by Run 1 ATLAS searches. Taken from Ref. [35].

LSP exclusion extends up to approximately 900 GeV, corresponding to a gluino mass of approximately 1450–1600 GeV. The ATLAS exclusion limits obtained with the full $\sqrt{s} = 8$ TeV dataset are also shown. The new results represent a large improvement over the Run 1 limits.

4. Third generation squark direct production searches

This section presents several results from third generation squark (stop and sbottom) direct production searches using first $\mathscr{L} = 3.2$ fb^{-1} dataset at $\sqrt{s} = 13$ TeV. Production of these sparticles is considered separately from other ATLAS SUSY searches, as they are expected to have a more moderate cross section than the gluinos and first and second generation squarks. The decays of these particles also produce a large number of jets, possibly leptons, and $E_{\mathrm{T}}^{\mathrm{miss}}$. Large missing transverse momentum is important in defining the signal regions as well as the tagging of jets from b-quarks.

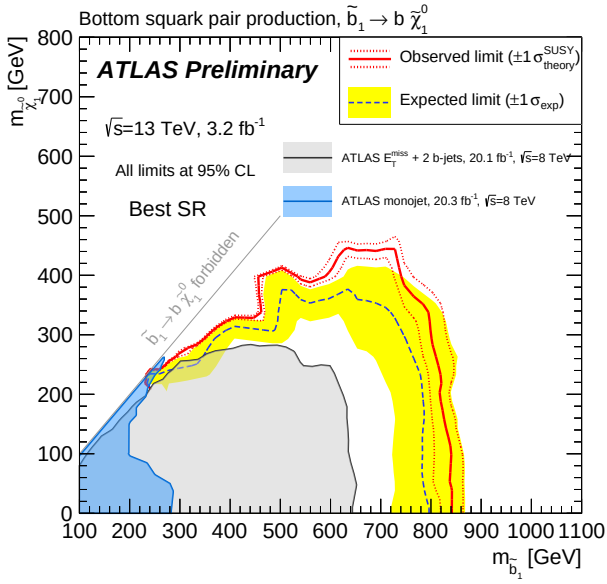

Fig. 8. 95% C.L. exclusion limits for direct bottom squark pair production with respect to the bottom squark mass ($m_{\tilde{b}_1}$) and to the neutralino mass ($m_{\tilde{\chi}_1^0}$). Results are compared with the observed limits obtained by Run 1 ATLAS searches. Taken from Ref. [34].

A search for pair production of the supersymmetric partner of the SM bottom quark ($\tilde{b}_1$) has been performed in events characterized by the presence of up to four jets, exactly two of which were identified as originating from a b-quark and large $E_{\mathrm{T}}^{\mathrm{miss}}$ [34]. Figure 3 (c) shows the topology of

the phenomenological supersymmetric models considered, in which the $\tilde{b}_1$ is the lightest squark. The rise in the production cross section of the studied signal processes is due to the increase of the centre-of-mass energy of the pp collisions in Run 2 of the LHC. For instance, for a $\tilde{b}_1$ with mass of 800 GeV, the production cross section increases by almost a factor of 10 going from $\sqrt{s} = 8$ TeV to $\sqrt{s} = 13$ TeV. The signal regions are defined to provide sensitivity to the kinematic topologies arising from different mass splittings between the bottom squark and the neutralino. No excess above the expected SM background yields is observed. Therefore, exclusion limits at 95% C.L. on the mass of the bottom squark are derived. Figure 8 shows the observed and expected exclusion limits at 95% C.L. in the $m_{\tilde{b}_1}$–$m_{\tilde{\chi}_1^0}$ plane. Also shown are the results obtained using Run 1 dataset. Bottom squark masses up to 800 (840) GeV are excluded for $\tilde{\chi}_1^0$ mass below 360 (100) GeV. Differences in mass above 100 GeV between the $\tilde{b}_1$ and the $\tilde{\chi}_1^0$ are excluded up to $\tilde{b}_1$ masses of 500 GeV. The new results extend the constraints on bottom squark mass by more than 150 GeV with respect to the $\sqrt{s} = 8$ TeV limits despite the lower integrated luminosity because of the increase in centre-of-mass energy of the LHC.

5. Electroweak production searches

This section presents searches for electroweak direct production of SUSY particles (charginos, neutralinos) using $\mathscr{L} = 20.3$ fb^{-1} dataset at $\sqrt{s} = 8$ TeV. Even though the gluinos and squarks are produced strongly in pp collisions, if the masses of the gluinos and squarks are large, the direct production of charginos, neutralinos and sleptons through electroweak interactions may dominate the production of SUSY particles at the LHC. Direct production of charginos and neutralinos, considering the $\tilde{\chi}_1^0$ as LSP, is expected to have a clean signature due to the presence of SM bosons and leptons in the decay chains and often low hadronic activity. Depending on the mass splitting, a heavier neutralino can decay to the LSP via slepton, Z or Higgs boson, and the charginos via slepton or W boson.

The ATLAS results for electroweakino searches in the framework of simplified models are summarized in Fig. 9 in the $m_{\tilde{\chi}_1^\pm,\tilde{\chi}_2^\pm,\tilde{\chi}_3^\pm}$–$m_{\tilde{\chi}_1^0}$ plane [36]. Each of the $\tilde{\chi}_1^\pm/\tilde{\chi}_2^\pm/\tilde{\chi}_3^\pm$ decays considered in the plot is assumed to have 100% branching fraction, and the production cross section is for pure wino $\tilde{\chi}_1^\pm\tilde{\chi}_1^\pm$ and $\tilde{\chi}_1^\pm\tilde{\chi}_2^0$ and pure higgsino $\tilde{\chi}_2^0\tilde{\chi}_3^0$. For $\tilde{\chi}_1^\pm\tilde{\chi}_1^\pm$ production with slepton-mediated decays, $\tilde{\chi}_1^\pm$ masses up to 500 GeV are excluded. In the $\tilde{\chi}_1^\pm\tilde{\chi}_2^0$ and $\tilde{\chi}_2^0\tilde{\chi}_3^0$ scenarios with slepton-mediated decays, $\tilde{\chi}_1^\pm$ and $\tilde{\chi}_2^0$ masses are excluded up to 700 GeV and 670 GeV respectively. For all three slepton-mediated decay scenarios, the value of the slepton mass is not seen to have a significant effect on the sensitivity.

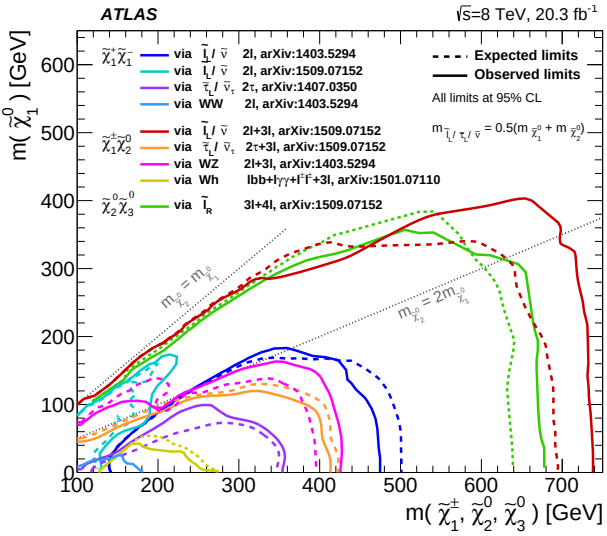

Fig. 9. The 95% C.L. exclusion limits for direct $\tilde{\chi}_1^{\pm}\tilde{\chi}_1^{\pm}$, $\tilde{\chi}_1^{\pm}\tilde{\chi}_2^0$, and $\tilde{\chi}_2^0\tilde{\chi}_3^0$ pair production with either SM-boson-mediated or slepton-mediated decays, as a function of the $\tilde{\chi}_1^{\pm}$, $\tilde{\chi}_2^0$, $\tilde{\chi}_3^0$ masses ($m_{\tilde{\chi}_1^{\pm},\tilde{\chi}_2^0,\tilde{\chi}_3^0}$) and $\tilde{\chi}_1^0$ mass ($m_{\tilde{\chi}_1^0}$). Taken from Ref. [36].

A search for the same-sign chargino-pair production via vector boson fusion (VBF) with subsequent slepton mediated chargino decays into final states with two the same-sign light leptons, at least two jets and $E_{\mathrm{T}}^{\mathrm{miss}}$ has been performed [36]. Scenarios with small mass splittings between $\tilde{\chi}_1^{\pm}$ and $\tilde{\chi}_1^0$ (so-called compressed SUSY spectra) are investigated. The illustration of $\tilde{\chi}_1^{\pm}\tilde{\chi}_1^{\pm}$ production via VBF, where the sparticles are produced along with two jets, is shown in Fig. 6 (c). The jets are widely separated in pseudo-rapidity and have a relatively high dijet invariant mass. Due to the VBF topology, the charginos are often boosted in the transverse plane, forcing the decay products to be more collinear and energetic, even in highly compressed spectra. Although the cross section for VBF production is significantly lower than that for direct production, those features of VBF production make it a good candidate to probe compressed SUSY scenarios that are experimentally difficult to explore via the direct production modes. This analysis is the first in ATLAS to search for SUSY particles production via VBF. Observation of such a process would prove that the exchanged neutralino is a Majorana particle. No significant excess of events beyond SM expectations is observed. Figure 10 shows the 95% C.L. upper limits on the cross section for $m(\tilde{\chi}_1^{\pm}) = 120$ GeV, as a function of the mass splitting between the chargino and the neutralino. The best observed upper limit on the VBF $\tilde{\chi}_1^{\pm}\tilde{\chi}_1^{\pm}$ production cross section is found for a mass splitting of 25 GeV, where the theoretical cross section at LO is 4.3 fb and the 95% C.L. upper limit on the cross section is 10.9 fb.

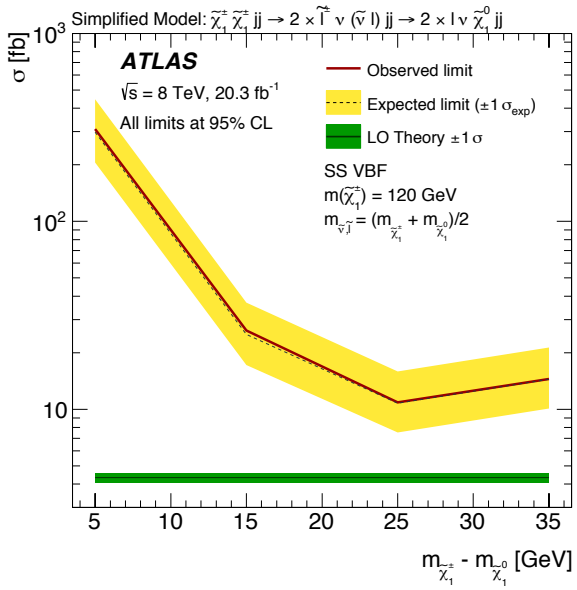

Fig. 10. The 95% C.L. upper limit on the cross section for the same-sign $\tilde{\chi}_1^\pm \tilde{\chi}_1^\pm$ pair production via VBF for $m_{\tilde{\chi}_1^\pm} = 120$ GeV. The limits have been set with respect to the mass difference between $\tilde{\chi}_1^\pm$ and $\tilde{\chi}_1^0$ ($m_{\tilde{\chi}_1^\pm} - m_{\tilde{\chi}_1^0}$). Taken from Ref. [36].

6. pMSSM interpretation

This section summarises the combined sensitivity and constraints from 22 separate ATLAS analyses of the Run 1 LHC dataset [37]. The interpretation of those results is done here within the wider framework of the pMSSM, where the over a hundred parameters of the MSSM are reduced to 19 applying a series of assumptions motivated by either experimental constraints or general features of possible SUSY breaking mechanisms. In this section, the model is assumed to conserve R-parity and the LSP is assumed to be the lightest neutralino. A total of 310,327 model points are selected, each of which satisfies constraints from previous collider searches, precision measurements, cold dark matter energy density measurements and direct dark matter searches.

The impact of the ATLAS Run 1 searches on this model space is presented in Fig. 11, showing their overall effect in constraining such supersymmetric models. The plot shows the fraction of model points excluded for each sparticle as a function of the sparticle mass.

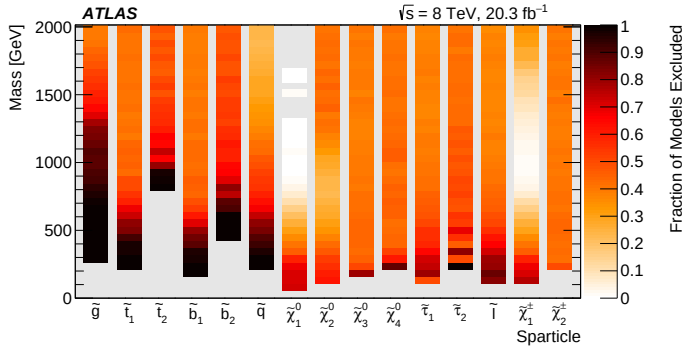

Fig. 11. Fraction of model points excluded for each sparticle as a function of the sparticle mass in pMSSM interpretation of Run 1 data. Taken from Ref. [37].

7. Conclusions

The ATLAS experiment at the LHC is conducting a comprehensive set of searches for supersymmetry exploiting different signatures and using various detection techniques. We have presented a summary of some of searches, based on a $\mathscr{L} = 3.2$ fb^{-1} Run 2 dataset of $\sqrt{s} = 13$ TeV proton–proton collisions recorded in 2015. Also, examples of the rich variety of Run 1 results at $\sqrt{s} = 7$ and 8 TeV using a total integrated luminosity up to $\mathscr{L} = 20.3$ fb^{-1} recorded are highlighted. Having found no evidence of signal in data, 95% C.L. exclusion limits on cross sections and masses have been expanded, thus continuing to constrain the parameter space of many physics models. However, an interesting excess corresponding to 2.2 standard deviations has been observed in the events containing a leptonically decaying Z boson, jets and $E_{\mathrm{T}}^{\mathrm{miss}}$. Much of the parameter space remains to be probed, and the search for SUSY at the LHC will continue. In particular, the LHC Run 2, which has already started, presents holds a potential for discovery of new physics due to its higher center-of-mass energy and luminosity.

REFERENCES

[1] H. Miyazawa, *Prog. Theor. Phys.* **36**, 1266 (1966).
[2] Y.A. Golfand, E.P. Likhtman, *JETP Lett.* **13**, 323 (1971).
[3] J. Gervais, B. Sakita, *Nucl. Phys. B* **34**, 632 (1971).
[4] P. Ramond, *Phys. Rev. D* **3**, 2415 (1971).
[5] A. Neveu, J.H. Schwarz, *Nucl. Phys. B* **31**, 86 (1971).
[6] A. Neveu, J.H. Schwarz, *Phys. Rev. D* **4**, 1109 (1971).
[7] D.V. Volkov, V.P. Akulov, *Phys. Lett. B* **46**, 109 (1973).

[8] J. Wess, B. Zumino, *Nucl. Phys. B* **70**, 39 (1974).
[9] J. Wess, B. Zumino, *Nucl. Phys. B* **78**, 1 (1974).
[10] J. Wess, B. Zumino, *Phys. Lett. B* **49**, 52 (1974).
[11] S. Ferrara, B. Zumino, *Nucl. Phys. B* **79**, 413 (1974).
[12] A. Salam, J.A. Strathdee, *Phys. Lett. B* **51**, 353 (1974).
[13] P. Fayet, *Phys. Lett. B* **64**, 159 (1976).
[14] P. Fayet, *Phys. Lett. B* **69**, 489 (1977).
[15] G.R. Farrar, P. Fayet, *Phys. Lett. B* **76**, 575 (1978).
[16] P. Fayet, *Phys. Lett. B* **84**, 416 (1979).
[17] S. Weinberg, *Phys. Rev. D* **13**, 974 (1976).
[18] E. Gildener, *Phys. Rev. D* **14**, 1667 (1976).
[19] L. Susskind, *Phys. Rev. D* **20**, 2619 (1979).
[20] N. Sakai, *Zeit. Phys. C* **11**, 153 (1981).
[21] S. Dimopoulos, S. Raby, F. Wilczek, *Phys. Rev. D* **24**, 1681 (1981).
[22] L.E. Ibanez, G.G. Ross, *Phys. Lett. B* **105**, 439 (1981).
[23] S. Dimopoulos, H. Georgi, *Nucl. Phys. B* **193**, 150 (1981).
[24] S. Weinberg, *Phys. Rev. D* **19**, 1277 (1979).
[25] A. Djouadi, J.L. Kneur, G. Moultaka, *Comput. Phys. Commun.* **176**, 426 (2007).
[26] C.F. Berger *et al.*, *J. High Energy Phys.* **0902**, 023 (2009).
[27] M.W. Cahill-Rowley *et al.*, *Eur. Phys. J. C* **72**, 2156 (2012).
[28] ATLAS Collaboration, *JINST* **3**, S08003 (2008).
[29] L. Evans, P. Bryant, *JINST* **3**, S08001 (2008).
[30] ATLAS Collaboration, *Eur. Phys. J. C* **72**, 1849 (2012).
[31] ATLAS Collaboration, ATLAS-CONF-2015-062 (2015), `https://cds.cern.ch/record/2114828`
[32] ATLAS Collaboration, *Phys. Lett. B* **757**, 334 (2016) [`arXiv:1602.06194 [hep-ex]`].
[33] ATLAS Collaboration, ATLAS-CONF-2015-082 (2015), `https://cds.cern.ch/record/2114854`
[34] ATLAS Collaboration, ATLAS-CONF-2015-066 (2015), `https://cds.cern.ch/record/2114833`
[35] ATLAS Collaboration, ATLAS-CONF-2015-067 (2015), `https://cds.cern.ch/record/2114839`
[36] G. Aad *et al.* [ATLAS Collaboration], *Phys. Rev. D* **93**, 052002 (2016).
[37] ATLAS Collaboration, *J. High Energy Phys.* **1510**, 134 (2015).